INTERNATIONAL JOURNAL OF HYDROGEN ENERGY XXX (2015) 1–8

Available online at www.sciencedirect.com

ScienceDirect

journal homepage: www.elsevier.com/locate/he

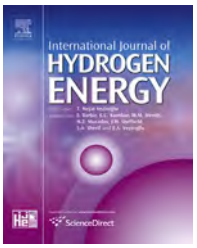

Sheet sensor using $SrAl_2O_4$:Eu mechanoluminescent material for visualizing inner crack of high-pressure hydrogen vessel

Yuki Fujio [a,*], Chao-Nan Xu [a,b,*], Yujin Terasawa [a], Yoshitaro Sakata [a], Junichiro Yamabe [b,c], Naohiro Ueno [d], Nao Terasaki [a], Akihito Yoshida [a], Shogo Watanabe [e], Yukitaka Murakami [f]

[a] Advanced Manufacturing Research Institute, National Institute of Advanced Industrial Science and Technology (AIST), Saga 841-0052, Japan

[b] International Institute for Carbon-Neutral Energy Research (WPI-I^{2}CNER), Kyushu University, Fukuoka 819-0395, Japan

[c] International Research Center for Hydrogen Energy, Kyushu University, Fukuoka 819-0395, Japan

[d] Department of Advanced Technology Fusion Graduate School of Science and Engineering, Saga University, Saga 840-8502, Japan

[e] Hydrogen Energy Test and Research Center, Fukuoka 819-1133, Japan

[f] Emeritus, Kyushu University, Fukuoka 819-0395, Japan

ARTICLE INFO

Article history:
Received 4 August 2015
Received in revised form
9 October 2015
Accepted 19 October 2015
Available online xxx

Keywords:
Mechanoluminescent materials
Elasticoluminescence
Hydrogen storage cylinder
Inner crack visualization
Nondestructive evaluation technique

ABSTRACT

A new non-destructive evaluation technique to detect cracks emanating from the inner surface (inner cracks) of a high-pressure hydrogen storage cylinder was developed by means of mechanoluminescence (ML) sensor consisting of $SrAl_2O_4$:Eu ML material and epoxy resin. To visualize the inner crack, a sheet ML sensor was attached onto the outer surface of the storage cylinder subjected to hydraulic pressure cycling with the maximum pressure of 45 MPa. The ML pattern was changed with an increase in the cycle number and the ML sensor could visualize the inner crack. The stress analysis by the finite element method clarified that the ML sensor provided unique equivalent strain distribution associated with stress concentration at the crack tip, i.e. the distance between two points having high equivalent strains was inversely proportional to the crack depth; consequently, the growth behavior of the inner crack was non-destructively quantified with the ML sensor attached on the outer surface.

* *Corresponding authors*. Advanced Manufacturing Research Institute, National Institute of Advanced Industrial Science and Technology (AIST), Saga 841-0052, Japan. Fax: +81 942 81 3696.

E-mail addresses: yuki-fujio@aist.go.jp (Y. Fujio), cn-xu@aist.go.jp (C.-N. Xu).

http://dx.doi.org/10.1016/j.ijhydene.2015.10.073

Please cite this article in press as: Fujio Y, et al., Sheet sensor using $SrAl_2O_4$:Eu mechanoluminescent material for visualizing inner crack of high-pressure hydrogen vessel, International Journal of Hydrogen Energy (2015), http://dx.doi.org/10.1016/j.ijhydene.2015.10.073

Introduction

Hydrogen has been considered as one of the most promising energy carriers because of its environmentally clean characteristic, high efficiency, and low pollutant emission [1–4]. Furthermore, the hydrogen plays an important role in a green energy, because it can be generated from the electrolysis of water using the renewable energy sources, such as wind-, water-, and solar-based technologies [5–7]. Recently, the first hydrogen fuel cell vehicle for personal use has been commercialized and the necessary hydrogen filling stations are gradually being built in the world. In the hydrogen filling stations, metallic or carbon fiber reinforced plastic (CFRP) composite storage cylinders are used to store the high-pressure gaseous hydrogen [8–11]. However, the use of hydrogen poses serious safety issues [12]. For example, the hydrogen can dissolve into some kind of metals or alloys, resulting in the leakage of hydrogen or unexpected failure associated with hydrogen embrittlement [7–10,13–15]. In order to ensure the safety in the hydrogen-based society, a non-destructive evaluation technique to sense invisible damages such as hydrogen-assisted fatigue cracks emanating from an inner surface of a storage cylinder is strongly required.

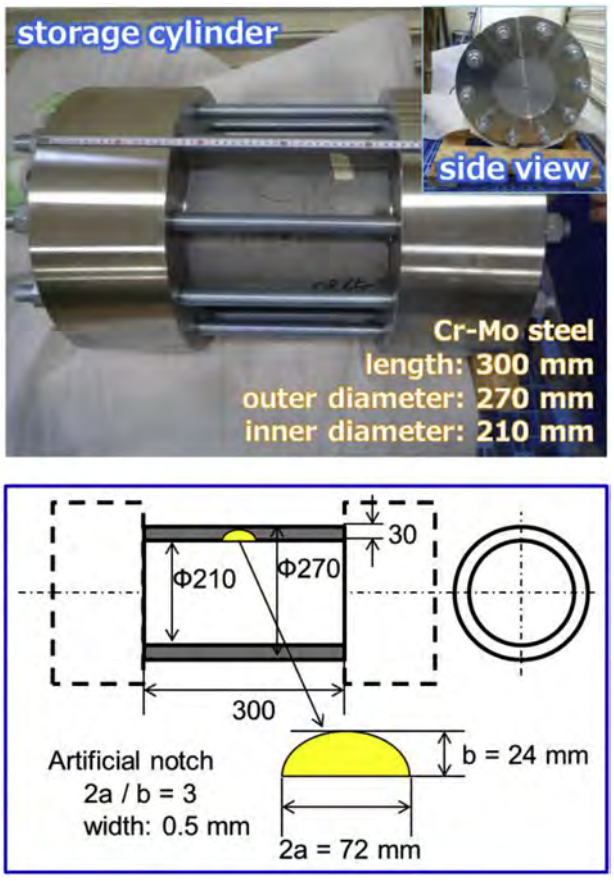

Fig. 1 – Photograph and schematic illustration of storage cylinder used in this study.

The development of safe, reliable, and cost-effective non-destructive evaluation technique is one of the most technically challenging subjects. So far, there have been some reports in regard to the non-destructive evaluation techniques to detect inner cracks produced in a high-pressure storage cylinder [16], such as ultrasonic [17,18], acoustic emission [19,20], thermography [21], and magnetic testing [22]. In recent years, we have developed and reported a new-type structural health monitoring technique using mechanoluminescence (ML) materials for bridge, building, pipe, and so on [23–28]. The ML material emits intensive light repeatedly accompanied by mechanical actions including deformation, friction, and impact even in elastic deformation range, and also the light intensity is proportional to strain energy of the material [29–35]. Such a phenomenon is classified into elasticoluminescence. Thus, using the ML material as a non-destructive evaluation technique, the strain distribution of an object is observed via the ML light intensity distribution. Actually, there has been an increasing number of reports about non-destructive evaluation techniques utilizing ML material [23–28,35–37].

As advantages of a technique using the ML material (ML sensor) compared with other techniques, we can say that the ML sensor provides the simple measurement system only using ML sensor and cameras for recording ML emission pattern. Additionally, the obtained ML emission patterns exhibit a two-dimensional mechanical information (strain distribution), indicating that the stress concentration and crack growth can be visualized in real time without the

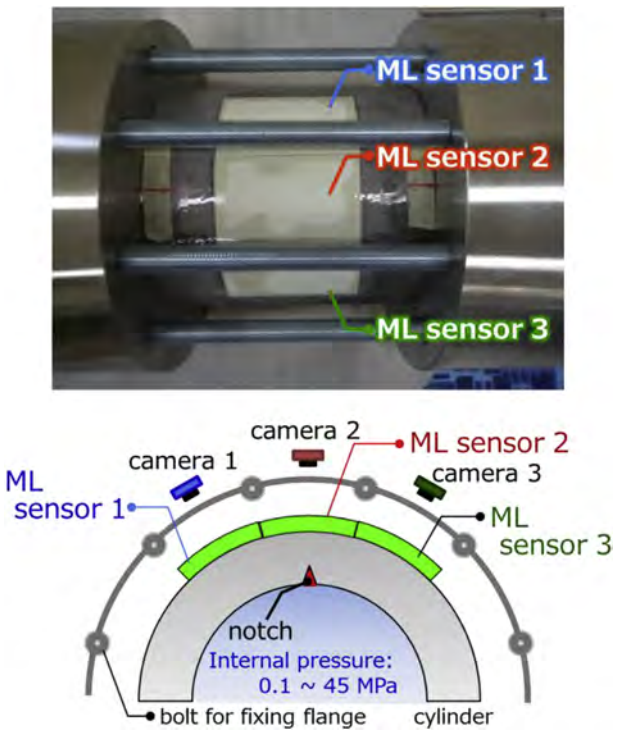

Fig. 2 – Photograph of storage cylinder attached with three ML sensors and schematic view of ML image monitoring system.

Please cite this article in press as: Fujio Y, et al., Sheet sensor using $SrAl_2O_4$:Eu mechanoluminescent material for visualizing inner crack of high-pressure hydrogen vessel, International Journal of Hydrogen Energy (2015), http://dx.doi.org/10.1016/j.ijhydene.2015.10.073

complicated analysis. The other inspections such as ultrasonic and acoustic emission need enormous cost and time, because they need thousands of locations, and they also need the complicated signal analysis. The ML technique provides a novel way of diagnosing the structural health, especially in early detection for safe and security measurement. In previous works, we have reported that ML sensor, which consists of a mixture of ML material and epoxy resin, putting on outer surface could visualize the inner crack of a storage cylinder made of manganese steel, and the magnitude of equivalent strain was estimated through the ML intensity, to be the ML intensity based monitoring method on inner crack growth [38]. However, it is practically difficult to measure the accurate ML intensity repeatedly for monitoring under changeable environmental light condition in outdoor such as hydrogen filling station. Therefore, for practical monitoring and prediction of aged deterioration focusing on the inner crack growth, non-destructive evaluation technique not based on ML intensity remains challenging.

In this study, we applied polymer composite films (ML sensor) made of the ML material and epoxy resin to a non-destructive evaluation technique to detect an inner crack in a high-pressure hydrogen storage cylinder. Specifically, we explored a possibility of the ML sensor as a new technique for visualizing inner cracks of a Cr–Mo steel cylinder with an artificial notch under hydraulic pressure cycling. As a result, the developed ML sensor was found to be in a usable way for the non-destructive evaluation technique to visualize the inner cracks in the high-pressure hydrogen storage cylinder. The detailed results and the inspection mechanism are reported and discussed here.

Experimental

Mechanoluminescent sensor

We selected europium doped strontium aluminate ($SrAl_2O_4$:Eu, SAOE) as an ML material in the ML sheet sensor, because it shows the highest ML intensity enough to be seen by the naked eye [30–32,39]. The SAOE powder was prepared by using a solid-state reaction method, which is the same as those previously reported [23–27]. Commercial $SrCO_3$, α-Al_2O_3, Eu_2O_3, and small amount of Ho_2O_3 powders were mixed in an agate mortar. The obtained mixture was calcined at 800 °C for 1 h in an atmospheric air; subsequently, was sintered at 1350 °C for 4 h in a reducing atmosphere (H_2+Ar) to synthesize the SAOE powder. The ML sheet sensors were fabricated by using a mixture of the pulverized SAOE powder and epoxy resin under screen-printing technique. The pulverized SAOE powder and epoxy resin were mixed thoroughly in a plastic cup, and then epoxy curing agent was added and mixed. The obtained SAOE paste was defoamed in vacuum desiccator for 10 min. The resulting paste was screen-printed on an aluminum sheet and subsequently dried until the SAOE film was fully solidified. The thickness of the SAOE film was controlled to be approximately 80 μm. Finally, the SAOE film was cut in a rectangular shape of 80*130 mm to fabricate three ML sheet sensors.

Storage cylinder sample

A photograph and schematic configuration of the storage cylinder (Cr–Mo steel, JIS-SCM435) are shown in Fig. 1. The chemical composition of the Cr–Mo steel was C 0.37 mass%, Si 0.21 mass%, Mn 0.77 mass%, P 0.012 mass%, S 0.007 mass%, Cr 1.07 mass%, and Mo 0.28 mass%: the remainder was Fe. This steel was oil-quenched at 900 °C then tempered in air at 560 °C. The 0.2% proof stress and tensile strength in air were 782 MPa and 947 MPa, respectively. The storage cylinder was made by cutting the sides of 35-MPa class stationary storage cylinder prototype and the flanges were set at both ends of the storage cylinder. The physical dimensions of the storage cylinder were 300 mm in length; 210 and 270 mm inner and outer diameters, respectively. In this study, an artificial U-notch was introduced in the center of the storage cylinder as an internal crack, as shown in Fig. 1. The width and length of the artificial notch are 0.5 and 72 mm, respectively. The depth of the notch

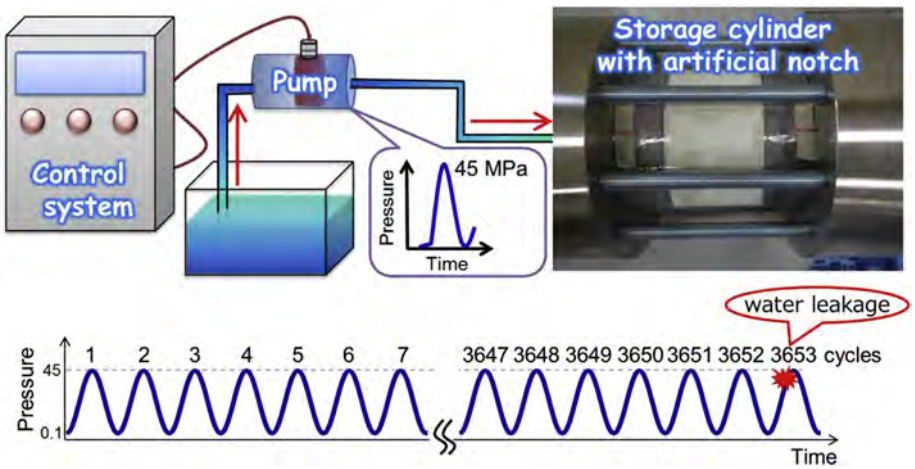

Fig. 3 – Schematic illustrations of experimental setup and time schedule of hydraulic pressure test.

Please cite this article in press as: Fujio Y, et al., Sheet sensor using $SrAl_2O_4$:Eu mechanoluminescent material for visualizing inner crack of high-pressure hydrogen vessel, International Journal of Hydrogen Energy (2015), http://dx.doi.org/10.1016/j.ijhydene.2015.10.073

is 24 mm (wall thickness: 30 mm). Three ML sheet sensors (80*130 mm in size) were attached onto the outer surface of the storage cylinder with a commercial adhesive (Fig. 2). The ML intensity distributions of ML sensors were recorded by using charge-coupled device (CCD) cameras at the frame rate of 5 frames per second (fps), as shown in Fig. 2. A three-axis strain gage was also attached to the outer surface of the storage cylinder by using a commercial adhesive to measure the strain of the outer surface.

Experimental setup

The fatigue testing of the storage cylinder was carried out by a hydraulic pressure tester at a W2 laboratory (Burst and endurance laboratory) in the Hydrogen Energy Test and Research Center (HyTReC), Japan. The experimental setup and time schedule of the hydraulic pressure test are drawn in Fig. 3. The internal pressure was cyclically varied from minimum pressure (atmospheric pressure) to maximum pressure (45 MPa) at a test frequency of 0.03 Hz. Before pressurizing the storage cylinder in the fatigue testing, the ML sheet sensors attached onto the outer surface of the storage cylinder were once irradiated by blue light-emitting diodes (LED) for 1 min and were kept under dark condition for 5 min to obtain reproducible and quantitative ML intensities. Such an experimental condition was decided on the basis of an ML mechanism (electron trapping mechanism) and our previous research [23–32]. With an increase in the internal pressure, the ML sensors emit light (ML) according to the dynamic deformation of the storage cylinder. The ML intensity distribution is simultaneously recorded as an image by CCD. The ML images were recorded at the 51st, 132nd, 237th, 2232nd, 2684th, and 3032nd cycle of the fatigue testing. In this fatigue testing, the storage cylinder with an artificial notch showed leak-before-break (LBB) at the 3653rd cycle.

Results and discussion

Fig. 4 shows ML images obtained from each of CCD cameras (cameras 1–3) corresponding to each of ML sensors (ML sensors 1–3) attached onto the outer surface of the storage cylinder at internal pressure of around 45 MPa in the 51st cycle of the fatigue testing. These ML images displayed a pseudo color image. The color of ML images varies from blue to red with the increase of ML intensity. As can be seen from Fig. 4, the ML images of ML sensors 1 and 3 exhibited pale lights in the entire field of the sensors, indicating that the storage cylinder deformed by the internal pressure of around 45 MPa. In actual, the strain gage attached to the outer surface of the storage cylinder, which locates at the opposite side of the inner artificial notch, showed the equivalent strain of about 700 μst when the internal pressure was around 45 MPa. On the contrary, the ML sensor 2, that is located over the inner artificial notch, gave the noticeable ML pattern. There are two points having higher ML intensity (green areas) in the center of the ML image compared to the surrounding area. This conspicuous ML pattern is presumed to be due to the artificial notch located at the inner surface of the storage cylinder. Fig. 5 shows the ML images of the ML sensor 2 at the internal pressure of around 45 MPa in the 132nd, 237th, 2232nd, 2684th, and 3032nd cycles of the fatigue testing. It can be also seen that the ML sensor 2 exhibited the conspicuous ML pattern in all of cycles. In addition, it should be noted that the ML

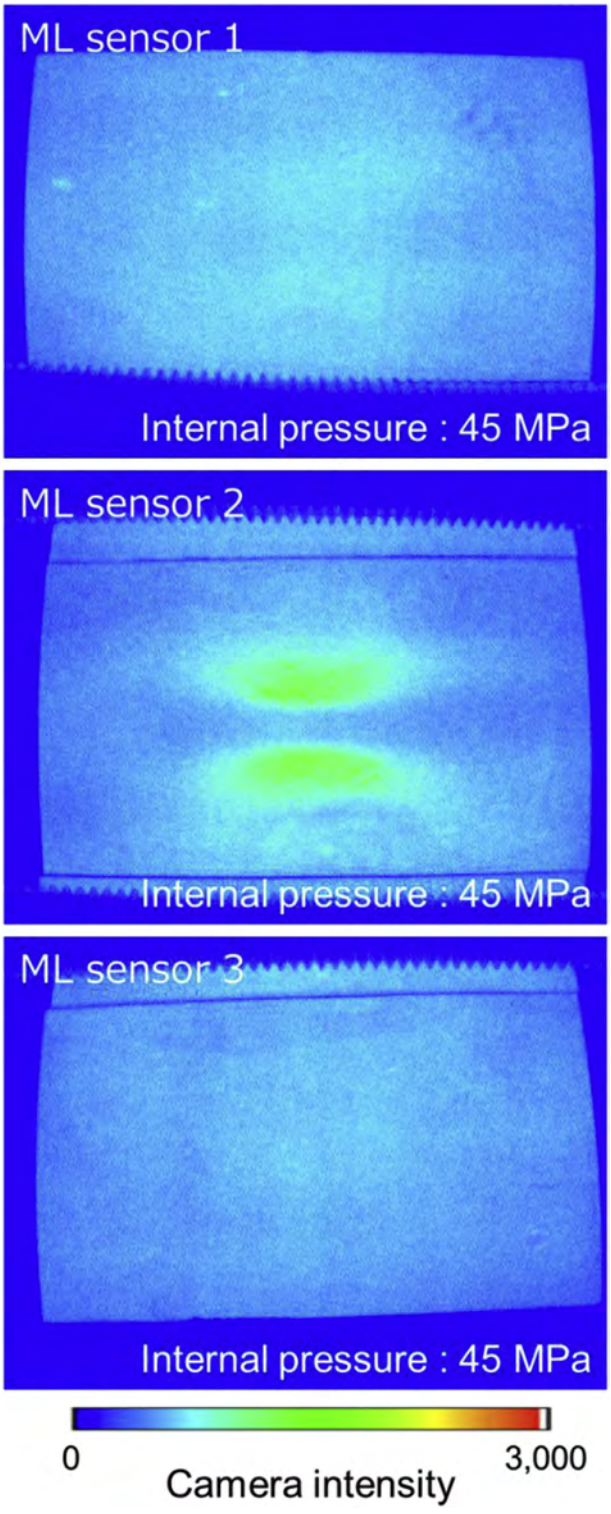

Fig. 4 – ML images obtained from each of ML sensors 1–3 attached to the outer surface of the storage cylinder at the internal pressure of around 45 MPa in the 51st cycle of fatigue testing.

Please cite this article in press as: Fujio Y, et al., Sheet sensor using $SrAl_2O_4$:Eu mechanoluminescent material for visualizing inner crack of high-pressure hydrogen vessel, International Journal of Hydrogen Energy (2015), http://dx.doi.org/10.1016/j.ijhydene.2015.10.073

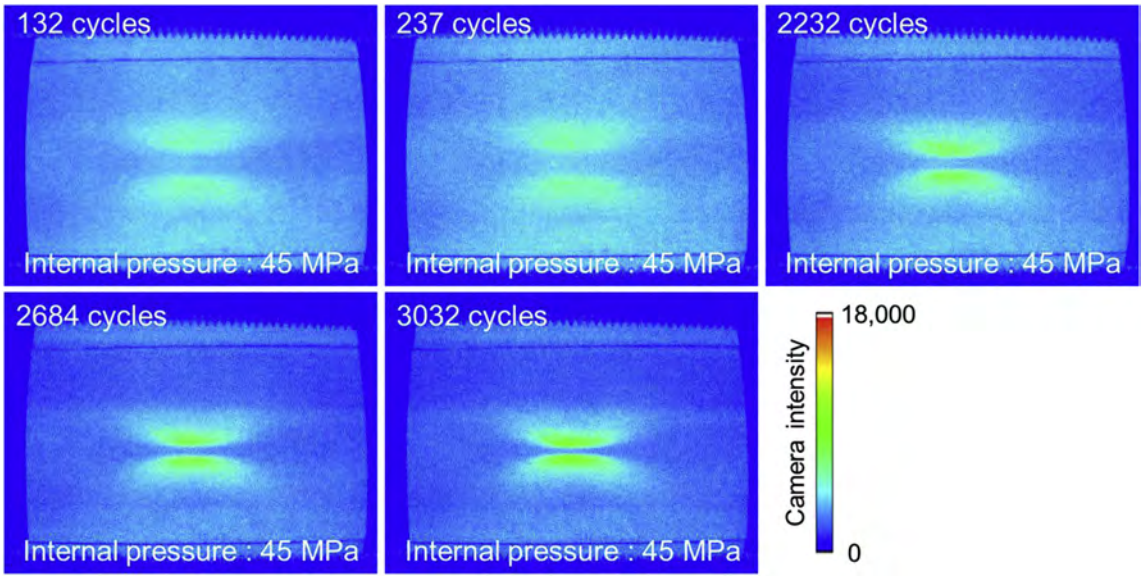

Fig. 5 – ML images obtained from ML sensor 2 attached to the outer surface of the storage cylinder at the internal pressure of around 45 MPa in the 132nd, 237th, 2232nd, 2684th, and 3032nd cycles of fatigue testing.

intensities in the center of ML image gradually increased with increasing the cycle number of fatigue testing as well as the distance between the two points with the higher ML intensities got gradually shorter and closed in on each other.

In order to investigate the reason for such a conspicuous change in the ML pattern, finite element method (FEM) calculations were carried out. The storage cylinder geometry has been built in a FEM model using computer code ANSYS. The FEM model including a crack reproduces real dimensions of the storage cylinder (Fig. 1) used in the fatigue testing. The length, inner radius, and outer radius of the storage cylinder constructed by the FEM model are 300, 210, and 270 mm, respectively. The length and width of the crack at the inner surface of FEM model were 72 and 0.5 mm, respectively. The depths of crack were set to 24.0, 25.5, 27.0, and 28.5 mm to investigate a change in an equivalent strain distribution toward fatigue crack propagation. The Young's modulus of 200 GPa and Poisson's ratio of 0.3 are adopted as elastic properties of the Cr–Mo steel. Tetrahedral solid elements constructed by four nodes and have six degrees of freedom (SOLID185) are employed. Fig. 6 shows three-dimensional model with meshes generated automatically using the ANSYS. The mesh size is made small in the vicinity of the crack. Fig. 7(a)–(d) shows cross-sectional view of the equivalent strain distribution surrounding the notch in the storage cylinder models with various crack depths (24.0–28.5 mm) at the internal pressure of 45 MPa calculated by FEM. From Fig. 7(a), it is clearly seen that there is stress concentration at the crack tip and the equivalent strain distribution is symmetric for the crack plane. The equivalent strain magnitude is the highest at the crack tip and gradually decreases with increasing distance from the crack tip. This phenomenon was commonly observed in the fatigue behavior [13,40–42]. With an increase in a crack depth (Fig. 7(b)–(d)), the equivalent strain distribution relevant to the stress concentration was shifted toward the outer surface of the storage cylinder. Thus, it was concluded that the equivalent strain distribution of the outer surface of the storage cylinder was related to the crack propagation, that is, the obtained ML images at the different cycle of fatigue testing (Fig. 5) show the equivalent strain distributions related to the crack propagation caused by the pressure cycling.

Fig. 8(a) shows the equivalent strain profile along A–A′ line in FEM calculation results (inset of Fig. 8(a)) at the internal pressure of 45 MPa for the storage cylinder models with different crack depths. For comparison, the ML intensity profiles along B–B′ line in ML images (inset of Fig. 8(b)) at the internal pressure of around 45 MPa in the different cycle numbers of fatigue testing were also presented in Fig. 8(b). In Fig. 8(a), it is seen that the distribution of the equivalent strains in the outer surface of the storage cylinder model with different crack depth is symmetric for the crack plane and

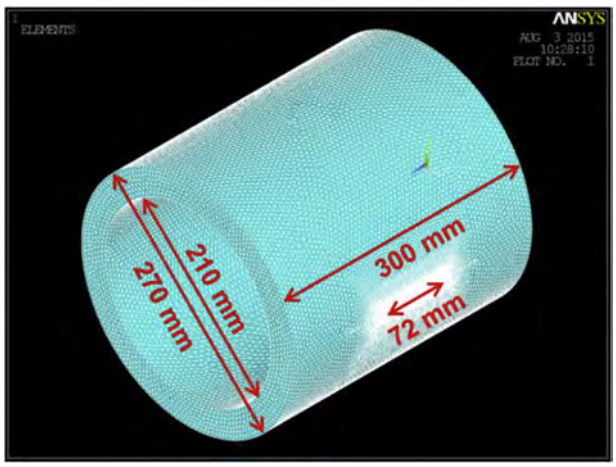

Fig. 6 – FEM model of storage cylinder with an artificial notch.

Please cite this article in press as: Fujio Y, et al., Sheet sensor using $SrAl_2O_4$:Eu mechanoluminescent material for visualizing inner crack of high-pressure hydrogen vessel, International Journal of Hydrogen Energy (2015), http://dx.doi.org/10.1016/j.ijhydene.2015.10.073

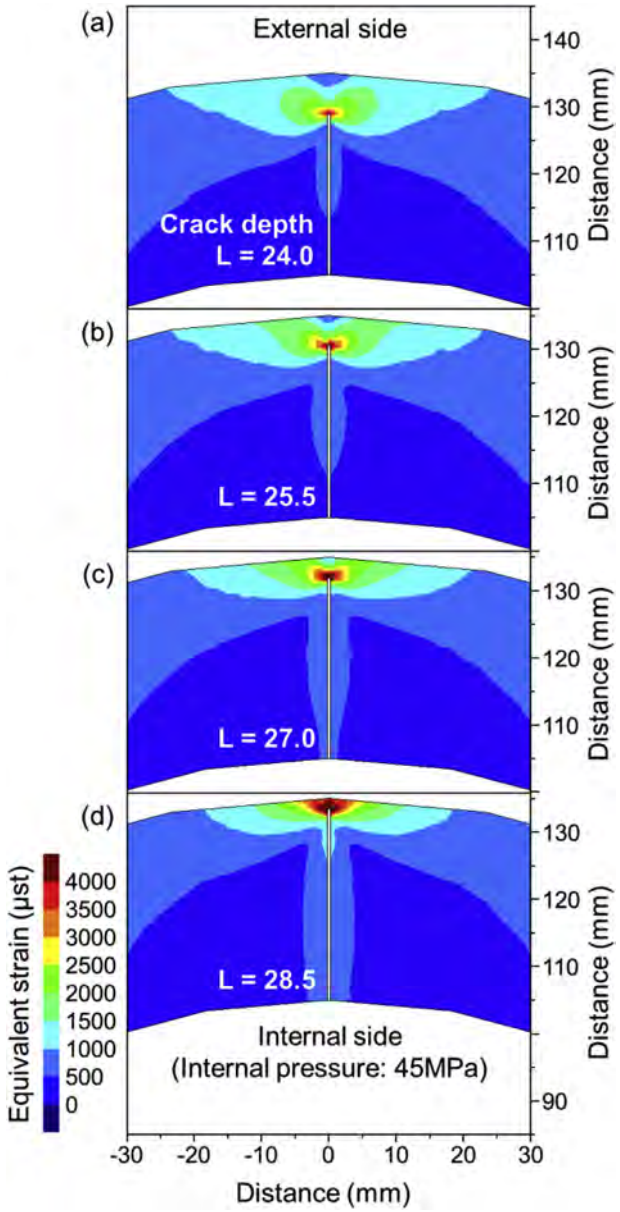

Fig. 7 – Cross-sectional view of the equivalent strain distribution calculated by FEM for storage cylinder models with different crack depth of (a) L = 24.0, (b) 25.5, (c) 27.0, and (d) 28.5 mm.

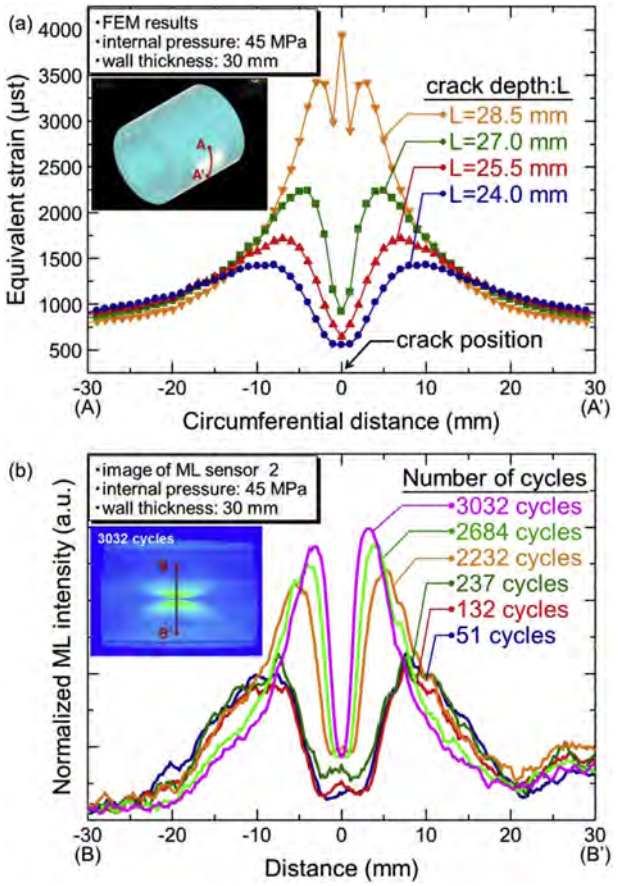

Fig. 8 – (a) Equivalent strain profiles along the circumference (A–A′ line in inset figure) of the storage cylinder model with various crack depths (24.0–28.5 mm) and (b) normalized ML intensity profiles along B–B′ line in inset ML image for the storage cylinder with the artificial notch, when the internal pressure of around 45 MPa was applied.

their strain magnitudes increase with increasing crack depth in the examined depth range of 24.0–28.5 mm. The obtained ML intensity profiles (Fig. 8(b)) were also demonstrated a similar behavior. Furthermore, it should be noted that the distance between two points having higher equivalent strain (Fig. 8(a)) is inversely proportional to the depth of the crack propagating from the inner surface of the storage cylinder, as shown in Fig. 9. Thus, we can speculate the crack depth by means of the distance between two higher strain points in the equivalent strain distribution of the outer surface of the storage cylinder. In order to verify the correlation between the crack depth and the distance between the higher equivalent strain points, the distances estimated by the experimentally

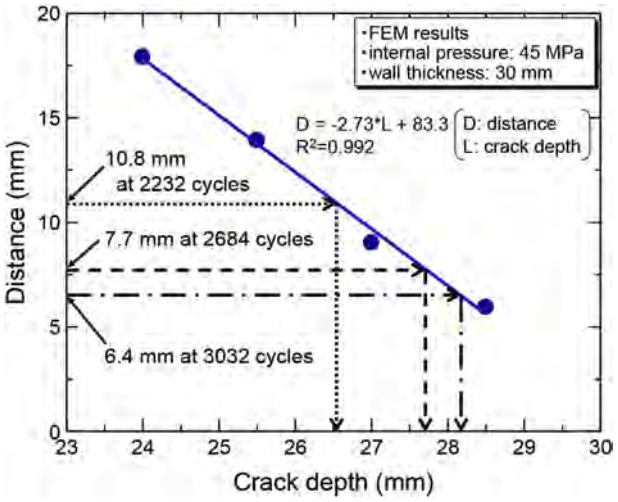

Fig. 9 – Dependence of the distance between two points having higher strain in the strain distribution calculated by FEM, on the crack depth of the inner surface of the storage cylinder at the internal pressure of 45 MPa.

Please cite this article in press as: Fujio Y, et al., Sheet sensor using $SrAl_2O_4$:Eu mechanoluminescent material for visualizing inner crack of high-pressure hydrogen vessel, International Journal of Hydrogen Energy (2015), http://dx.doi.org/10.1016/j.ijhydene.2015.10.073

Table 1 – Comparison of the distance between two higher ML intensities points in ML images and the distance between two higher equivalent strain points in FEM calculation results.

Experimental results of ML sensor		FEM calculation results	
Number of cycle	Estimated distance	Crack depth	Estimated distance
51	17.2		
132	17.6	24.0	17.9
237	17.4		

obtained ML images and the FEM calculation result at the initial crack depth (L = 24.0 mm) were presented in Table 1. It is clearly seen that the distances in the ML image at the 51st, 132nd, and 237th cycles, which seems to keep the artificial notch (24.0 mm), are in a good agreement with that at the crack depth of 24.0 mm obtained by the FEM calculation. This consistency reveals the correctness of the FEM calculations representing the distance in the ML image against the crack depth. Additionally, the distances in the ML image at the 2232nd, 2684th, and 3032nd cycles, were estimated to be about 10.8, 7.7, and 6.4 mm, respectively (Fig. 8(b)). From the relationship between the distance and crack length (Fig. 9), the crack lengths were speculated to be 26.6, 27.7, 28.2 mm in the 2232nd, 2684th, and 3032nd cycle, respectively. These results infer that observation by means of the ML images attached onto the outer surface of the storage cylinder can give information on the growth behavior of the crack located in the inner surface of the storage cylinder. Thus, the ML sensor is a promising candidate for the non-destructive evaluation technique to detect inner crack produced in a high-pressure hydrogen storage cylinder for the hydrogen filling stations.

Conclusions

A non-destructive evaluation technique by means of an ML sensor for detecting inner crack produced in a Cr–Mo steel storage cylinder for a hydrogen filling station was developed, and its sensing characteristics were investigated in a hydraulic pressure cycle test with the maximum pressure of 45 MPa. The ML sensor attached to the outer surface of the storage cylinder could visualize an artificial notch located in the inner surface. From the results of FEM calculation, a noticeable ML pattern was found to project an equivalent strain distribution relevant to a stress concentration at the crack tip. In addition, the distance between two points having the higher magnitude of equivalent strain was inversely proportional to the depth of the crack located in the inner surface of the storage cylinder. Thus, the developed ML sensor is manifest to be a promising candidate in regard to the non-destructive evaluation technique to detect inner cracks produced in a high-pressure storage cylinder for a hydrogen filing station.

Acknowledgments

The authors would like to thank the all member of ML team of AIST for their valuable discussions and help in the experiment.

This work was partially supported by Fukuoka Strategy Conference for Hydrogen Energy as well as Council for Science, Technology and Innovation (CSTI), Cross-ministerial Strategic Innovation Promotion Program (SIP), (Funding agency: JST).

REFERENCES

[1] Kruger P. Electric power requirement in the United States for large-scale production of hydrogen fuel. Int J Hydrogen Energy 2000;25:1023–33.
[2] Neelis ML, van der Kooi HJ, Geerlings JJC. Exergetic life cycle analysis of hydrogen production and storage systems for automotive applications. Int J Hydrogen Energy 2004;29(5):537–45.
[3] Aceves SM, Berry GD, Martinez-Frias J, Espinosa-Loza F. Vehicular storage of hydrogen in insulated pressure vessels. Int J Hydrogen Energy 2006;31(15):2274–83.
[4] Satyapal S, Petrovic J, Read C, Thomas G, Ordaz G. The U.S. Department of Energy's National hydrogen storage project: progress towards meeting hydrogen-powered vehicle requirements. Catal Today 2007;120:246–56.
[5] Kruk M, Jaroniec M. Gas adsorption characterization of ordered organic–inorganic nanocomposite materials. Chem Mater 2001;13(10):3169–83.
[6] Wang QK, Zhu CC, Liu WH, Wu T. Hydrogen storage by carbon nanotube and their films under ambient pressure. Int J Hydrogen Energy 2002;27(5):497–500.
[7] Bououdina M, Grant D, Walker G. Review on hydrogen absorbing materials-structure, microstructure, and thermodynamic properties. Int J Hydrogen Energy 2006;31(2):177–82.
[8] Nakamura J, Miyahara M, Omura T, Semba H, Wakita M, Otomea Y. Degradation of fatigue properties in high pressure gaseous hydrogen environment evaluated by cyclic pressurization tests. Proced Eng 2010;2:1235–41.
[9] Murakami Y, Matsuoka S. Effect of hydrogen on fatigue crack growth of metals. Eng Fract Mech 2010;77:1926–40.
[10] Macadre A, Yano H, Matsuoka S, Furtado J. The effect of hydrogen on the fatigue life of Ni-Cr-Mo steel envisaged for use as a storage cylinder for a 70 MPa hydrogen station. Int J Fatigue 2011;33:1608–19.
[11] Barthélémy H. Hydrogen storage – industrial prospectives. Int J Hydrogen Energy 2012;37:17364–72.
[12] Korotcenkov G, Han SD, Stetter JR. Review of electrochemical hydrogen sensors. Chem Rev 2009;109(3):1402–33.
[13] Murakami Y, Kanezaki T, Mine Y, Matsuoka S. Hydrogen embrittlement mechanism in fatigue of austenitic stainless steels. Metall Mater Trans A 2008;39:1327–39.
[14] Murakami Y, Kanezaki T, Mine Y. Hydrogen effect against hydrogen embrittlement. Metall Mater Trans A 2010;14:2548–62.
[15] Yamabe J, Matsumoto T, Matsuoka S, Murakami Y. A new mechanism in hydrogen-enhanced fatigue crack growth behavior of a 1900-MPa-class high-strength steel. Int J Fract 2012;177:141–62.
[16] Hufenbach W, Böhm R, Thieme M, Tyczynski T. Damage monitoring in pressure vessels and pipelines based on wireless sensor networks. Proced Eng 2011;10:340–5.
[17] Kobayashi M. Ultrasonic nondestructive evaluation of microstructural changes of solid materials under plastic deformation—Part II. Experiment and simulation. Int J Plast 1998;14(6):523–35.
[18] Kim C, Park I. Microstructural degradation assessment in pressure vessel steel by harmonic generation technique. J Nucl Sci Technol 2008;45(10):1036–40.

Please cite this article in press as: Fujio Y, et al., Sheet sensor using $SrAl_2O_4$:Eu mechanoluminescent material for visualizing inner crack of high-pressure hydrogen vessel, International Journal of Hydrogen Energy (2015), http://dx.doi.org/10.1016/j.ijhydene.2015.10.073

[19] Ohtsuka N, Nakano M, Ueyama H. Acoustic emission monitoring during rupture test of pressure vessels and laboratory fracture test. J Press Vessel Technol 1981;103:191–9.
[20] Ennaceur C, Laksimi A, Hervé C, Cherfaoui M. Monitoring crack growth in pressure vessel steels by the acoustic emission technique and the method of potential difference. Int J Press Vessels Pip 2006;83(3):197–204.
[21] Yang B, Liaw PK, Wang H, Jiang L, Huang JY, Kuo RC, et al. Thermographic investigation of the fatigue behavior of reactor pressure vessel. Mater Sci Eng A Struct 2001;314(1–2):131–9.
[22] Theiner WA, Reimringer B, Deimel P, Kuppler D, Schroeder-Obst D. Non-destructive analysis of the structure of pressure-vessel steels by micromagnetic testing techniques. Nucl Eng Des 1983;76(3):251–60.
[23] Li C, Xu CN, Zhang L, Yamada H, Imai Y. Dynamic visualization of stress distribution on metal by mechanoluminescence images. J Vis 2008;11(4):329–35.
[24] Ono D, Xu CN, Li C, Bu N. Visualization of internal defect of a pipe using mechanoluminescent sensor. J Jpn Soc Exp Mech 2010;10:152–6.
[25] Li C, Xu CN, Imai Y, Bu N. Real-time visualisation of the Portevin-Le Chatrlier effect with mechanoluminescent-sensing film. Strain 2011;47:483–8.
[26] Terasaki N, Xu CN, Li C, Zhang L, Li C, Ono D, et al. Visualization of active crack on bridge in use by mechanoluminescent sensor. Proc SPIE 2012;8348. 83482D-1–D-6.
[27] Terasaki N, Xu CN. Historical-log recording system for crack opening and growth based on mechanoluminescent flexible sensor. IEEE Sens J 2013;13(10):3999–4004.
[28] Ueno N, Xu CN, Watanabe S. Fatigue crack detection of CFRP composite pressure vessel using mechanoluminescent sensor. Proc IEEE Sensors 2013:1851–4.
[29] Xu CN, Watanabe T, Akiyama M, Zheng XG. Artificial skin to sense mechanical stress by visible light emission. Appl Phys Lett 1999;74:1236–8.
[30] Xu CN, Watanabe T, Akiyama M, Zheng XG. Direct view of stress distribution in solid by mechanoluminescence. Appl Phys Lett 1999;74:2414–6.
[31] Xu CN. In: Schwartz M, editor. Encyclopedia of smart materials, vol. 1. New York: John Wiley & Sons Inc.; 2002. p. 190–201.
[32] Liu Y, Xu CN. Influence of calcining temperature on photoluminescence and triboluminescence of europium-doped strontium aluminate particles prepared by sol-gel process. J Phys Chem B 2003;107(17):3991–5.
[33] Wang X, Xu CN, Yamada H, Nishikubo K, Zheng XG. Electro-mechano-optical conversions in Pr^{3+}-doped $BaTiO_3$-$CaTiO_3$ ceramics. Adv Mater 2005;17:1254–8.
[34] Terasaki N, Xu CN. Performance of single mechanoluminescenct particle as ubiquitous light source. J Colloid Interface Sci 2014;427:62–6.
[35] Wang X, Zhang H, Dong YL, Peng D, Zhang A, Zhang Y, et al. Dynamic pressure mapping of personalized handwriting by a flexible sensor matrix based on the mechanoluminescence process. Adv Mater 2015;27(14):2324–31.
[36] Kim JS, Kwon YN, Sohn KS. Dynamic visualization of crack propagation and bridging stress using the mechano-luminescence of $SrAl_2O_4$:(Eu,Dy,Nd). Acta Mater 2003;51:6437–42.
[37] Timilsina S, Lee KH, Kwon YN, Kim JS. Optical evaluation of in situ crack propagation by using mechanoluminesc-ence of $SrAl_2O_4$:Eu^{2+}, Dy^{3+}. J Am Ceram Soc 2015;98:2197–204.
[38] Guo S, Xu CN, Ono D, Li C, Sakata Y, Watanabe S. Visualization of the fatigue crack for pressure vessel by mechanoluminescence sensor. In: Proc. 2012 IEEE sensors applications symposium; 2012. p. 212–6.
[39] Xu CN, Yamada H, Wang X, Zheng XG. Strong elasticoluminescence from monoclinic-structure $SrAl_2O_4$. Appl Phys Lett 2004;84:3040–2.
[40] Robertson SW, Mehta A, Pelton AR, Ritchie RO. Evolution of crack-tip transformation zones in superelastic nitinol subjected to in situ fatigue: a fracture mechanics and synchrotron X-ray microdiffraction analysis. Acta Mater 2007;55:6198–207.
[41] Baxevanis T, Chemisky Y, Lagoudas DC. Finite element analysis of the plane strain crack-tip mechanical fields in pseudoelastic shape memory alloys. Smart Mater Struct 2012;21. 094012.
[42] Withers PJ. Fracture mechanics by three-dimensional crack-tip synchrotron X-ray microscopy. Philos Trans R Soc A 2013;373. 20130157.

Please cite this article in press as: Fujio Y, et al., Sheet sensor using $SrAl_2O_4$:Eu mechanoluminescent material for visualizing inner crack of high-pressure hydrogen vessel, International Journal of Hydrogen Energy (2015), http://dx.doi.org/10.1016/j.ijhydene.2015.10.073